SUPPLEMENTAL MATERIAL

Westerberg et al., http://www.jem.org/cgi/content/full/jem.20091245/DC1

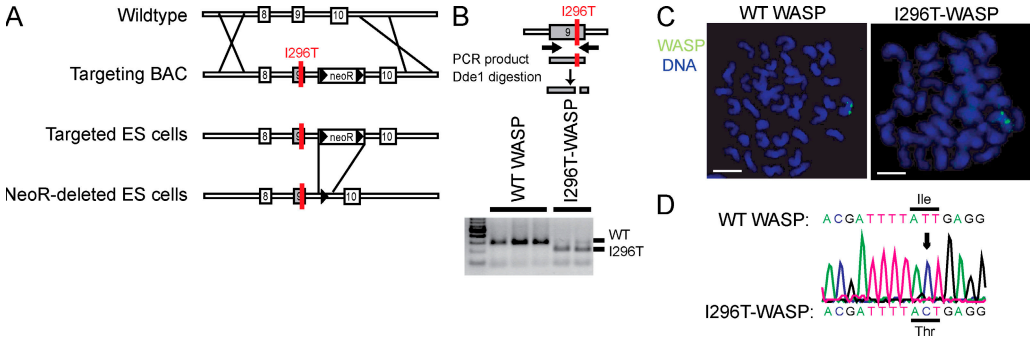

Figure S1. Targeting strategy and screening to generate WASP-I296T knockin ES cells. (A) A targeting construct was assembled by insertion of the WASP-I296T point mutation and an aph (neoR) cassette into a BAC containing the WASP gene. (B) PCR strategy to identify WASP-I296T–targeted ES cells. The WASP-I296T mutation introduces a unique restriction enzyme site recognized by *Dde1*. A 300-bp PCR product spanning the I296T mutation was generated followed by digestion with *Dde1*. The WT WASP allele is not recognized by *Dde1* and the PCR product remains 300 bp. The WASP-I296T allele is specifically digested to two new fragments by *Dde1*, 200 and 100 bp in length. *Dde1* digestion of three WT and two I296T-targeted ES cells is shown. (C) ES cell clones, positive using the PCR strategy, were further screened for homologous recombination by FISH. In WT and homologous-targeted ES cells, a BAC probe covering the WASP gene identifies two signals (green) representing the WASP locus on adjacent sister chromatids of the X chromosome during metaphase. DNA is labeled blue with DAPI staining. For nonhomologous targeted ES cells, the WASP probe identifies four signals: two representing the endogenous WASP locus and two representing nonhomologous targeting of the WASP BAC to another locus. The FISH analysis of one representative WT and one homologous-targeted WASP-I296T ES cell clone is shown. Bars, 1 µm. (D) Sequence analysis of a representative positive ES cell clone confirmed the T to C nucleotide mutation present in the homologous targeting of WASP-I296T ES cells.

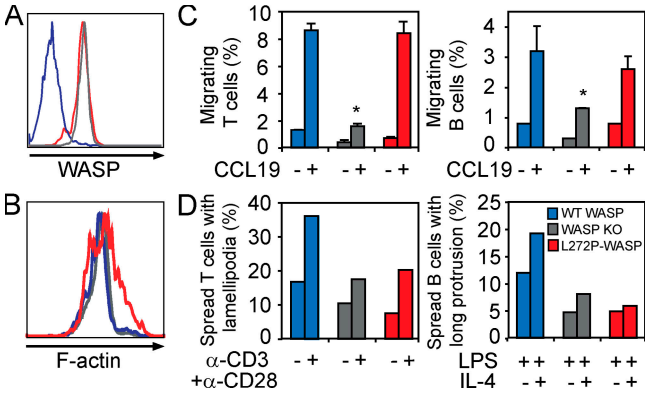

Figure S2. XLN-WASP-L272P gene therapy model: functional analysis of lymphocytes. (A) WASP expression. Lymph node T cells were stained for WASP using an anti-WASP antibody followed by flow cytometry analysis. The histogram is representative of at least three experiments. (B) F-actin content. Lymph node T cells were stained with phalloidin to detect F-actin and were analyzed by flow cytometry. The histogram is representative of three experiments. (C) Migration. Spleen lymphocytes were allowed to migrate to CCL19 for 3 h using an in vitro chemotaxis chamber. Migrating cells were collected and enumerated by flow cytometry with reference beads. The percentage of migrating cells is shown as mean values (±SD) of triplicates and is representative of at least three experiments. *, $P < 0.05$ compared with WT. (D) Spreading. (left) Spreading of T cells was assessed on anti-CD3 plus anti-CD28 antibody–coated surfaces (right). Spreading of B cells was assessed on anti-CD44 antibody–coated surfaces. Graphs show the percentage of spread T (left) and B cells (right) representative of at least three experiments.

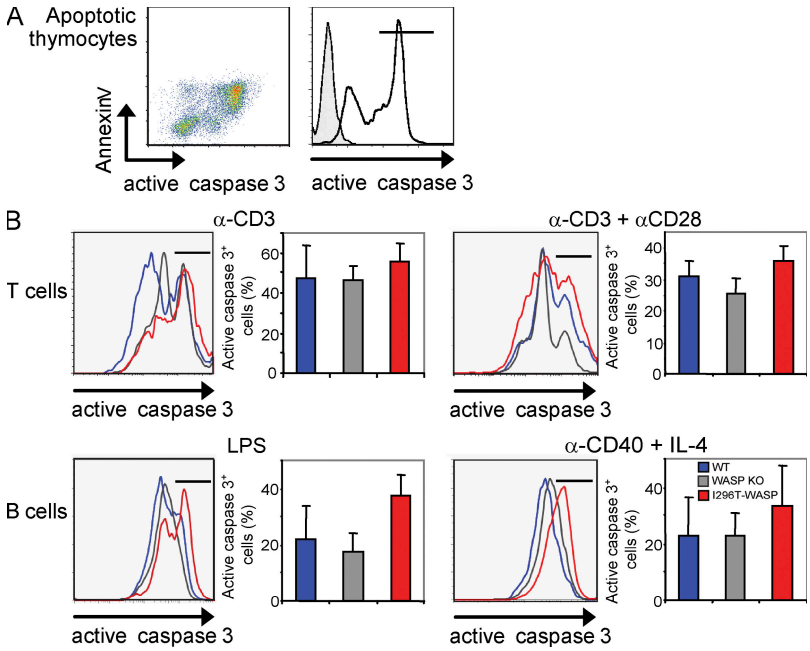

Figure S3. Increased apoptosis of WASP-I296T B and T cells detected by anti-active caspase-3 staining. (A) Staining to detect active caspase-3. To confirm that the anti-active caspase-3 antibodies recognized apoptotic cells, dexamethasone-treated apoptotic thymocytes were stained for cell-surface annexin V and intracellulary for active caspase-3 and analyzed by flow cytometry. A large percentage of thymocytes are annexin V^{high}active caspase-3^{high} apoptotic cells. The histogram (right) shows thymocytes positive for active caspase-3 (continuous line) as compared with the isotype control (shaded). The horizontal bar denotes active caspase-3^+ cells. (B) Apoptosis. Spleen T and B cells were stimulated with the indicated stimulus for 72 h. The percentage of apoptotic cells was assessed after labeling with anti-active caspase-3 antibodies and flow cytometric analysis. Apoptotic cells were defined as active caspase-3^{high}. Each panel shows one representative histogram (left) and one graph of mean values (±SD) of analysis of cells from three mice (right). This experiment represents one out of two similar experiments.